

A bulk 2D Pauli Limited Superconductor

T. Coffey,¹ C. Martin,¹ C. C. Agosta,¹ Tatsue Kinoshota,² and M. Tokumoto^{3,2}

¹*Department of Physics, Clark University, Worcester, MA, 01610*

²*CREST, JST, Kawaguchi 332-0012 Japan*

³*Nanotechnology Research Institute, AIST, Tsukuba 305-8568, Japan*

(Dated: February 7, 2020)

We present a nearly perfect Pauli limited critical field phase diagram for the anisotropic organic superconductor $\alpha\text{-}(\text{ET})_2\text{NH}_4(\text{SCN})_4$ when the applied magnetic field is oriented parallel to the the conducting layers. The phase diagram matches calculations published by Klemm, Luther, and Beasley (Phys. Rev. B **12**, 877 (1975)) very well. The critical fields were found by using a tunnel diode oscillator to measure the penetration depth. Because the critical field, H_{c2} , is Pauli limited, we can calculate the size of the superconducting energy gap based on the maximum H_{c2} . We also discuss the role of spin orbit scattering and many body effects on our results.

PACS numbers: 74.70.Kn, 74.25.Dw

There have been many theoretical calculations and experiments on layered superconductors when an external magnetic field is applied parallel to the conducting layers [1, 2, 3, 4, 5, 6, 7, 8, 9]. If the conducting layers are precisely aligned with the applied field, the magnetic flux lines normally present in a type II superconductor pass between the conducting planes of a highly anisotropic superconductor, and the orbital destruction of superconductivity associated with the vortices is suppressed. In this orientation the interaction of the Cooper pairs can be studied more directly because the bound state of the pairs will be broken when the Zeeman energy is equal to the superconducting energy gap. This limit, where the Cooper pairs are separated due to the external magnetic field, is known as the Clogston-Chandrasekar or Pauli paramagnetic limit [11]. A clean superconductor that is Pauli limited is also a good candidate for other exotic superconducting states such as the Fulde-Ferrell-Larkin-Ovchinnikov state (FFLO) [9].

Previous attempts to create a bulk model Pauli limited superconductor, have been unsuccessful due to insufficient anisotropy or spin orbit scattering [12]. However, a convincing Pauli limited superconductor was realized for a single layer of aluminum [13]. The organics are very good candidates for reaching the Pauli limit in a bulk superconductor because they are lower dimensional conductors and clean. These properties have led to a number of theoretical and experimental studies that investigated the anisotropic properties of quasi one- and two-dimensional organic conductors. Some of the interesting phenomena include reentrant superconductivity [6, 7], vortex lockin [8], dimensional crossover [14], and the FFLO state [15]. $\alpha\text{-}(\text{ET})_2\text{NH}_4(\text{SCN})_4$ [ET-NH4] is one of the most anisotropic of the organic conductors and very clean samples are available. For comparison, the anisotropy parameter γ for ET-NH4 = 2000, while $\gamma=150$ for $\text{Bi}_2\text{Sr}_2\text{CaCu}_2\text{O}_{8+\delta}$ (BiSCCO) [31]. The mean free path in ET-NH4 is 680 Å, while the mean free path in BiSCCO is less than 100 Å. The T_c of ET-NH4 is 0.96 K

and its superconducting coherence lengths are: $\xi_{||} = 628$ Å and $\xi_{\perp} \leq 25$ Å.

In this letter we present a Pauli limited critical field phase diagram for the anisotropic organic superconductor ET-NH4. The phase diagram is a close match to the calculations done by Klemm, Luther, and Beasley (KLB) [1] in the limit of small spin-orbit scattering. Or one could claim that Bulaevskii's paper [4] is more appropriate because it addresses clean superconductors, but the results are very similar. Both theories may be valid, because the coherence length of ET-NH4 puts it on the cusp of the clean and dirty limit. Our phase diagram is based on rf penetration depth measurements, which have been used to characterize several superconductors [18, 19].

In our measurements the sample is placed in a small coil that is part of a self resonant circuit. The sample is placed with its flattest side on a rotating platform so that the conducting planes of the sample are perpendicular to the platform and the axis of the coil as shown in Fig. 1. The coil excites rf currents in the conducting planes of the sample due to the rf field generated by the coil which is $< 70 \mu\text{T}$. Small balls of cotton are packed between the sample and the coil and a Teflon gurney is tied around the coil and the rotating platform to hold the sample in place. In one of the data runs presented in this letter, a small dot of Apiezon N grease was applied to hold the sample in place. The critical fields found from the different runs agree, implying that the stresses induced in the sample by the grease did not affect the critical fields. All measurements were done on the same single crystal, although between each of the three experimental runs, the sample cracked and lost about 10% of its volume [40]. The initial size of the crystal was 1.69 mm by 1.83 mm by 1.0 mm. The measurements were conducted using a transverse 1 T electromagnet at Clark University and a 18 T superconducting magnet at the NNMFL. At Clark University the angular resolution is 0.1°. The angular resolution at the NNMFL was limited to 0.05° because the angle was changed by hand instead of a servomotor.

The axis of rotation of the platform is along one diagonal of the ac plane of the sample.

The rf penetration depth in superconductors has been discussed by many authors [8, 16, 20]. In type II superconductors the normal skin depth δ , the London penetration depth λ_L , and the Campbell penetration depth λ_C combine to form a complex penetration depth that is proportional to the surface impedance of the sample $Z_S = R_S + iX_S$. Below H_{c2} , R_S and X_S are proportional to the imaginary and real parts of the penetration depth [20, 21]. As the field is increased, the flux lattice is melted and λ_L diverges at H_{c2} according to

$$\lambda_L = \frac{\lambda_L(0)}{(1 - H/H_{c2})^{\frac{1}{2}}}, \quad (1)$$

and the penetration depth becomes limited by δ . Above H_{c2} , if the skin depth is much less than the size of the sample, the sample reactance X_S and sample resistance R_S will be equal. This regime is often called the skin depth limit [23].

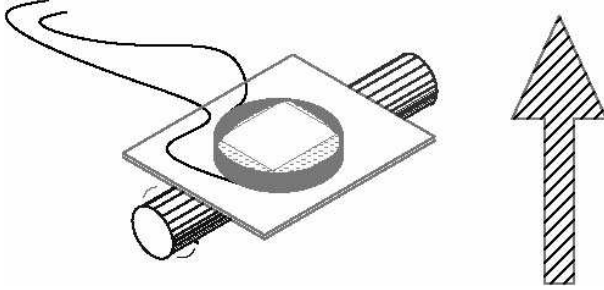


FIG. 1: This is a schematic of the coil and sample on a rotating platform. The large arrow indicates the direction of the applied field. The cylinder is the axis of rotation.

In a TDO experiment we measure the amplitude and frequency of a self-resonant circuit. These quantities are determined by the complex impedance $j\omega L$ of the coil containing the sample. A long rod in a uniaxial coil changes the inductance of the coil according to [22],

$$L' = L_0 (1 + 4\pi\eta\{\chi' - j\chi''\}), \quad (2)$$

where η is defined as the volume filling factor. As the rf field is expelled from the sample, the filling factor changes. However, our samples are small blocks and Eq. (2) must be corrected by a demagnetization factor that depends on the geometry of the sample and coil. Demagnetization factors for several geometries of normal and superconducting materials can be calculated [17, 23, 24] and several experimental techniques have been tested to measure the demagnetization factor [16, 25].

In general, $\Delta F/F_0 \propto X_S$ and $\frac{1}{A} \propto R_S$, where Z_{tc} is the impedance of the tank circuit. For a metallic

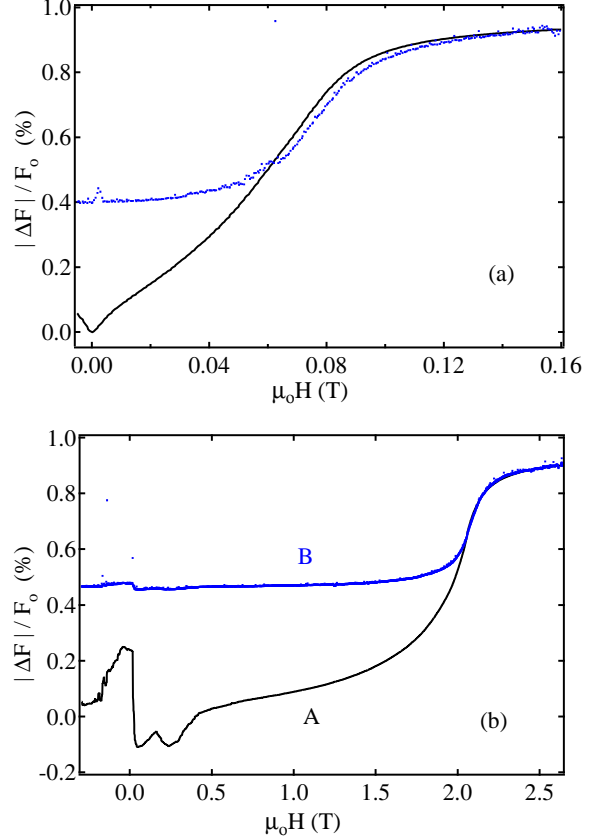


FIG. 2: Comparison of frequency shift $\frac{\Delta F}{F_0}$ and inverse amplitude data $\frac{1}{A}$ versus applied field. The absolute value of the amplitude data depends upon the amplification and is arbitrary. (a) The applied field is perpendicular to the conducting planes; $T \approx 200$ mK. $\frac{\Delta F}{F_0}$ is represented by the solid line. $\frac{1}{A}$ is represented by the dots. At low fields $\frac{\Delta F}{F_0}$ is clearly $\propto \sqrt{H}$ and $\frac{1}{A}$ bottoms out. (b) The applied field is parallel and $T \approx 80$ mK. $\frac{\Delta F}{F_0}$ is labelled A and $\frac{1}{A}$ is labelled B. The frequency shift is clearly not $\propto \sqrt{H}$ and $\frac{1}{A}$ bottoms out at an applied field close to the superconducting transition.

sample in the skin depth regime, $X_S = R_S$ and therefore, $\Delta F/F_0 \propto \frac{1}{Z_{tc}}$. In our experiments the frequency changes by $< 1\%$ in contrast to the amplitude signal which can change by a large percentage ($\approx 50\%$). These shifts are different because the change in frequency is proportional to the change in the inductance of the tank circuit, $\frac{\Delta F}{F_0} \approx \frac{\Delta L}{2L_0}$ and the amplitude signal is directly proportional to the impedance of the tank circuit. There is, however, a limit when Z becomes greater than $|R_n|$, (where R_n is the negative resistance of the tunnel diode) when the TDO no longer oscillates. Near this limit the change amplitude does become nonlinear. Above this limit the change in frequency (the reactive part) in our experiments is small, and the amplitude signal, $\propto \frac{1}{Z_{tc}}$ is inversely proportional to the resistive or loss mechanisms

in the coil and sample, so that, $A \propto Z_{tc} \propto \frac{1}{R_{\text{sample}} + R_{\text{coil}}}$.

We have not measured the demagnetization factor and do not report absolute penetration depths, but the superconducting transition is clear in our data. λ_L and δ place our experiments in the skin depth limit where the dominant mechanism is a change in the filling factor or penetration depth. This limit is consistent with our data where the amplitude and frequency change in an almost identical manner near and above the superconducting transition and with other measurements of λ_L [31]. In Fig. 2a the applied field is perpendicular to the conducting layers and $\frac{\Delta F}{F_0} \propto \sqrt{H}$ at low fields, which is consistent with the Campbell penetration region. There is very little low field structure in the amplitude signal. In the parallel orientation, Fig. 2b, we observe no \sqrt{H} behavior at low fields in the frequency signal. Instead, we observe large hysteretic behavior in the frequency signal. We believe the hysteretic behavior is related to some kind of non-equilibrium flux dynamics.

H_{c2} is found by finding the maximum in the second derivative of the frequency response of the TDO with respect to the applied field. This method and extrapolating a straight line through the data above and below the superconducting transition produce a consistent H_{c2} . Preliminary results from the NHMFL showed a surprising flat HT phase diagram at low temperatures as shown in Fig. 3, which did not agree with either of the two previously published results [26, 27] for this phase diagram (which crossed, and initially motivated our experiment). Because the low temperature data taken at the NHMFL was unexpected, we conducted a second run using a different circuit in the same 18 T magnet. The data from these and our Clark runs are consistent. To insure that the parallel critical fields are accurate, seven

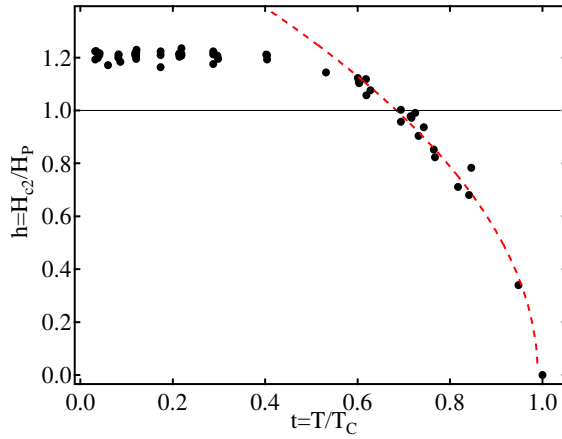


FIG. 3: The phase diagram plotted in reduced coordinates. $h = \frac{H_{c2}}{H_P^{\text{BCS}}}$. $t = \frac{T}{T_c}$. The dashed line is a fit to the data where $h \propto \sqrt{1-t}$. The solid line indicates H_P^{BCS} .

full angular studies were conducted between 40 mK and

700 mK. H_{c2} as a function of angle at 40 mK is plotted in Fig. 4a. A comparison between the data and the predictions for a layered superconductor in the 2D and 3D limiting cases is made in Fig. 4b at angles close to the parallel orientation. The low temperature data fits very well to Eq. (3) which indicates that the vortices in each layer are decoupled and ET-NH4 is a two-dimensional superconductor [5]. We note that this theory does not account for the fact that ET-NH4 is Pauli limited, although we expect the Pauli limit will only change the results very close ($< 1^\circ$) from the parallel orientation.

$$\left| \frac{H_{c2}(\theta) \cos(\theta)}{H_{c2\perp}} \right| + \left[\frac{H_{c2}(\theta) \sin(\theta)}{H_{c2\parallel}} \right]^2 = 1. \quad (3)$$

To clarify our main points, the phase diagram is plotted in reduced coordinates, where $t = \frac{T}{T_c}$, $h = \frac{H_{c2}}{H_P^{\text{BCS}}}$, and H_P^{BCS} is the Pauli limit in the context of the BCS theory. Temperature sweeps indicate $T_c = 0.96$ K which is very close to previously reported values [28, 29, 30, 31]. If H_{c2} is Pauli limited, $H_{c2}(T)$ should be directly proportional to the superconducting energy gap, and if we assume that ET-NH4 is a BCS superconductor, $\mu_0 H_P^{\text{BCS}} = 1.84 T_c = 1.77$ T (where 1.84 has the units of T/K). There are two striking features in Fig. 3: The low temperature critical fields appear saturated at 2.15 T, 20% above H_P^{BCS} , and the critical fields near T_c are proportional to the approximate BCS equation for the gap energy near T_c : $\Delta \propto (1-t)^{\frac{1}{2}} \propto H_{c2}$. It is clear that our phase diagram follows the same functional form as the energy gap, albeit with $H_{c2}(0) > H_P^{\text{BCS}}$.

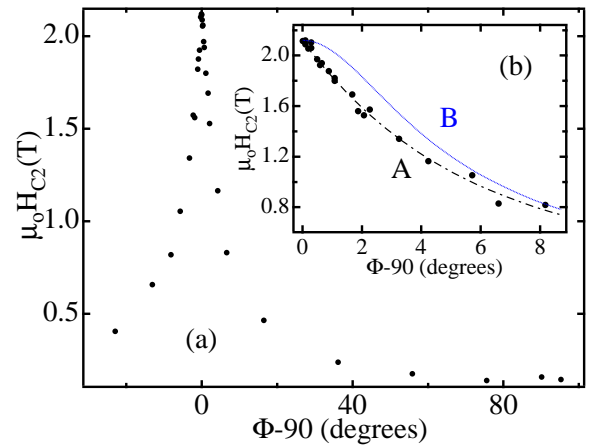


FIG. 4: (a) H_{c2} as a function of angle at 40 mK. (b) The dashed-dotted line is a fit to Eq. (3) and the solid line is a fit to the anisotropic Ginzburg Landau theory. The angle(θ) between the normal of the conducting layer and the applied field is zero when the applied field is perpendicular to the conducting layers.

Three possible mechanisms can enhance the Pauli

limit: stronger coupling, many body effects, or spin-orbit scattering. The coupling constant $\alpha = 1.76$ for a BCS superconductor. α would have to be equal to 2.16 if stronger coupling were responsible for the higher H_{c2} in ET-NH4, but specific heat data show that if anything, α is less than 1.76 [34]. Mckenzie has shown that many body effects can increase the Pauli limit by a factor of $\frac{1}{R}$, where R is Wilson's ratio. Wilson's ratio for ET-NH4 is 0.7 ± 0.2 or 0.86 ± 0.05 (depending on the experimental data used) as calculated in Ref. [33]. Zou et al. proposed a theory independent method to estimate the many body enhancement [35]. This method equates the condensation energy of the superconductor and the energy gained by having the electrons' spin align with the applied field. Using the jump in specific heat data [28, 29, 31] to estimate the condensation energy and susceptibility [32], we followed Zou's method to estimate the renormalization of the Pauli limit. Zou's method depends on which set of specific heat data is used, and produces a high and low estimate very similar to the many body theory using Wilson's ratio. In both cases the low estimates predict a Pauli limit 20% higher than H_P^{BCS} which agrees with our phase diagram.

A third mechanism that can enhance H_P is spin-orbit scattering. KLB calculate $\frac{H_{c2}}{H_P}$ as a function of temperature for many different rates of spin-orbit scattering for layered superconductors with a field applied parallel to the layers. In a system with no spin-orbit scattering, H_{c2} saturates near the Pauli limit. Systems with higher spin-orbit scattering rates are shown to reach 2 to 6 times the Pauli limit. The flat temperature dependence of our data at low temperatures and the moderate enhancement of the critical field over the BCS prediction qualitatively place our data between a system with no spin-orbit scattering and one with a spin-orbit scattering time of 5.0 ps. If one assumes that all of the enhancement of H_{c2} is due to spin orbit scattering, Eq. (4) from KLB can be used to estimate a spin-orbit scattering time $\tau_{\text{so}} = 12.6$ ps in ET-NH4.

$$H_{c2}(0) = 0.602(\tau_{\text{so}}T_C)^{-1/2}H_P^{\text{BCS}}. \quad (4)$$

The total scattering rate in the metallic state can be obtained by measuring the decay of quantum oscillations as a function of applied field [36, 37]. The total scattering rate is usually reported as a Dingle temperature T_D where $\tau = \hbar/(2\pi k_b T_D)$. The reported T_D for ET-NH4 ranges from 0.6 K [38] to 1.4 K [39] with most samples having a T_D closer to 1.4 K. We measured Shubnikov de Haas oscillations when the applied field is perpendicular to the conducting planes at seven temperatures between 39 mK and 706 mK. From this data we find an effective mass of $2.5 m_e$ and a T_D of 1.11 K which is consistent with the previously reported values. This Dingle temperature implies a scattering time of 1.09 ps.

The spin-orbit scattering times are much longer than the measured scattering time, suggesting that the spin-orbit scattering is not the dominant scattering mechanism. We also could assume that both many body effects and spin orbit scattering play a part in driving up the critical field.

The last possibility is that the FFLO state exists above the line we define as H_{c2} , and we are not sensitive to the phase line between the FFLO state and the normal metallic phase. Careful specific heat measurements with accurately aligned samples could determine if an exotic state existed beyond what we measure as H_{c2} or not.

We would like to acknowledge H. Gao, J. Norton, T. Murphy, E. Palm and S. Hannahs for help doing these experiments, R. Klemm for useful discussions, and NSF grant #9805784 for support. We would also like to thank L. Rubin for donated equipment from the FBNML.

- [1] R. A. Klemm et al., Phys. Rev. B. **12**, 877 (1975).
- [2] D. Saint-James et al, *Type II Superconductivity*, Pergamon, Oxford (1969).
- [3] W. E. Lawrence and S. Doniach *Proceedings of the 12th International Conference on Low Temperature Physics*, ed. E. Kanada (Academic, Kyoto, Japan) (1971).
- [4] L. N. Bulaevskii, Sov. Phys. JETP **38**, 634 (1988).
- [5] T. Schneider and A. Schmidt, Phys. Rev. B **47**, 5915 (1993).
- [6] A. Lebed and K. Yamaji, Phys. Rev. Lett. **80**, 2697 (1998).
- [7] I. J. Lee et al., Phys. Rev. Lett. **78**, 3555 (1997).
- [8] P. Mansky et al., Phys. Rev. B **52**, 7554 (1995).
- [9] P. Fulde and R. A. Farrell, Phys. Rev. **135**, A550 (1964).
- [10] T. Ishiguro, Exactly Aligned High Magnetic Field Study of low-Dimensional Metals and Superconductors (2001), private communication.
- [11] A. M. Clogston, Phys. Rev. Lett. **9**, 266 (1962).
- [12] C. Strunk et al., Phys. Rev. B **49**, 4053 (1994).
- [13] P. M. Tedrow and R. Meservey, Phys. Rev. B **8**, 5098 (1973).
- [14] W. K. Kwok et al., Phys. Rev. B **42**, 8686 (1990).
- [15] M.-S. Nam, J. Phys. Cond. Matter **11**, L477 (1999).
- [16] S. Sridhar et al., Phys. Rev. Lett. **68**, 2220 (1992).
- [17] A. Omari and A. F. Khoder, Cryogenics **33**, 1098 (1993).
- [18] T. Coffey et al., Rev. Sci. Inst. **71**, 4600 (2000).
- [19] C. H. Mielke et al., J. Phys. -Condens. Mat. **13**, 8325 (2001).
- [20] M. W. Coffey and J. R. Clem, Phys. Rev. Lett. **67**, 386(1991).
- [21] M. W. Coffey and J. R. Clem, Phys. Rev.B **45**, 10, 527 (1992).
- [22] A. Abragam *The principles of Nuclear Magnetism*, Oxford University Press, (1961).
- [23] O. Klein et al., Int. J. of Infrared and Millimeter Waves **14**, 2423 (1993).
- [24] *Magnetic Susceptibility of Superconductors and Other Spin Systems*, ed. R. A. Hein, Plenum Press New York (1991).
- [25] R. Prozorov et al., Appl. Phys. Lett. **77**, 4202 (2000).
- [26] J. S. Brooks et al., Synth. Metals **70**, 839 (1995).

- [27] Y. Shimojo et al., *J. of Superconductivity* **12**, 501 (1999).
- [28] B. Andraka et al., *Phys. Rev. B* **42**, 9963 (1990).
- [29] Y. Nakazawa et al., *Phys. Rev. B* **52**, 12890 (1995).
- [30] H. H. Wang, *Physica C* **166**, 57 (1990).
- [31] H. Taniguchi et al., *Phys. Rev. B* **57**, 3623 (1998).
- [32] K. Miyagawa et al., *Synth. Metals* **86**, 1987 (1997).
- [33] R. H. Mckenzie, Los Alamos archive cond-mat/9905044 v2 (1999).
- [34] S. Wanka et al., *Phys. Rev. B* **57**, 3084 (1998).
- [35] F. Zuo et al., *Phys. Rev. B* **61**, 750 (2000).
- [36] D. Shoenburg *Magnetic Oscillations in Metals*, Cambridge University Press, (1984).
- [37] N. Harrison et al., *Phys. Rev. B* **52**, 5584 (1995).
- [38] J. Wosnitza et al., *Phys. Rev. B* **45**, 3018 (1992).
- [39] T. Osada et al., *Solid State Comm.* **75**, 901 (1990).
- [40] As this letter was being submitted, this experiment was repeated using a new sample from a different synthesis laboratory and we obtained identical results.